Evidence for Intramolecular Hydrophobic Association in Aqueous Solution for Pyrene-End-Capped Poly(ethylene oxide)

Jean Duhamel, Ahmad Yekta, Yong Zhong Hu, and Mitchell A. Winnik*

Erindale College and Department of Chemistry, University of Toronto, Toronto, Ontario, Canada M5S 1A1

Received April 6, 1992; Revised Manuscript Received September 8, 1992

ABSTRACT: Evidence is presented that in dilute aqueous solutions of a Py-PEO-Py polymer (Py = pyrene, PEO = poly(ethylene oxide)) (M_n = 8000, M_w/M_n = 1.08), 7% of the polymeric molecules exist in an end-associated conformation. When excited by UV light, dilute (less than 10^{-6} M) solutions of the polymer exhibit typical pyrene monomer and excimer fluorescence. The excimer fluorescence is shown to arise from intramolecular association only. Part of the excimer emission arises from diffusional approach and end-to-end cyclization during the lifetime of the excited pyrene monomer. The observation is that a significant portion of the excimer emission arises from direct UV excitation of polymers that exist in an intramolecularly end-associated conformation. We can make a clear distinction between excimers formed via diffusional end-to-end cyclization and direct excitation of associated end pairs by observing that selective quenching of the excited monomer leads to a decrease of the former type and not the latter. Spectral information, as well as dynamic and static quenching data, is presented to support this hypothesis. A kinetic model is developed, and rate parameters are extracted from data.

Introduction

Water-soluble polymers bearing hydrophobic substituents often have unusual properties in aqueous solution. In some instances they undergo intermolecular association to form multimolecular clusters which have a strong influence on solution viscosity. Associative thickeners,[1] used in paints, fall into this class of materials.

In other instances the nonpolar substituents undergo intramolecular association. Here one finds micelle-like domains inside the coil of individual polymer molecules.[2] Many factors affect the nature of the association process such as chain architecture and substituent length, number, and placement. Our understanding of these factors and how they operate remains rather limited.

Some insights come from very simple systems. The molecule pyrene-poly(ethylene oxide)-pyrene (Py-PEO-Py) is an example of a water-soluble polymer containing an excimer-forming dye at both ends of the chain.[3] In organic solvents it behaves "normally".[4] Upon pulsed excitation, the pyrene gives a blue monomer fluorescence of intensity $I_M(t)$, and as it decays, the green excimer emission $I_E(t)$ grows in and ultimately decays on the time scale of 1500 ns. This is the classic behavior expected for a random coil polymer with one pyrene excited which forms an excimer when the two chain ends diffuse together.[5] Since excimer formation is diffusion controlled, one is not suprised that the ratio of excimer and monomer fluorescence intensities, I_E/I_M, decreases with increasing solvent viscosity.

More than a decade ago we reported[6] that Py-PEO-Py gave significantly more excimer fluorescence in dilute solution in water than in any organic solvent, even those of lower viscosity. Time-resolved measurements indicated that much of the excimer was formed very rapidly, in less than 1 ns. This led to the suggestion of hydrophobic association between the pyrene end groups. The Frank group at Stanford took advantage of these properties and used these polymers as probes to study the complexation of hydrophobically modified PEO with poly(acrylic acid) and poly(methacrylic acid) in water.[7] At the same time they initiated a collaboration with Gast and co-workers to explore in more detail the nature of hydrophobic interactions in water.[8] In one particular paper,[8b] they proposed a model for the intramolecular hydrophobic interactions for Py-PEO-Py in water which we are now able to test. In addition Char, Gast, and Frank used these polymers to examine the interactions of PEO with the surface of silica particles in water.[9]

Here we return to the case of Py-PEO-Py in dilute aqueous solutions.[10] We report the synthesis and purification of the two polymers shown below, where the Py groups are attached by ether linkages so that they will not hydrolyze spontaneously in water. Comparison of the fluorescent properties of both molecules in water, particularly their susceptibility to fluorescence quenching by iodide ion, reveals an attractive and simple picture of the hydrophobic interaction between the two chain ends of Py-PEO-Py. Here a fraction of the ground-state molecules (α) are cyclized in water so that their Py end groups form a dimeric pair (D). Upon excitation, the dimeric pairs form excimers (D* → E*) in less than 1 ns. The remaining fraction (1 - α) are random coils. Upon excitation, these Py* groups form an excimer via the normal intramolecular diffusive process.

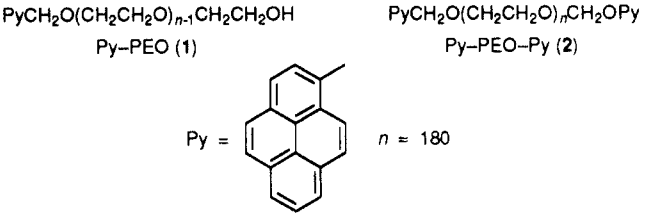

Experimental Section

Synthesis of the Labeled Polymer. 1-(Bromomethyl)-pyrene (3). 1-Pyrenemethanol (mp 112-114 °C) was obtained from the $NaBH_4$ reduction of pyrenecarboxaldehyde (Aldrich) in methanol. PBr_3 (0.88 mL in 5 mL of $CHCl_3$) was added dropwise under nitrogen to 1-pyrenemethanol (2.27 g) in chloroform (50 mL) containing pyridine (0.45 mL) while the temperature was kept close to 0 °C with an ice-water bath. The yellow mixture was allowed to warm to room temperature over 3.5 h. It was then poured onto ice, separated, dried (Na_2SO_4), and concentrated to yield a yellow powder, which was then recrystallized from benzene/cyclohexane (60/40) to yield 1.62 g (56%) of pale yellow cubic crystals (mp 145-147 °C).[11] This noxious material, a bad skin irritant, decomposes upon standing

0024-9297/92/2225-7024$03.00/0

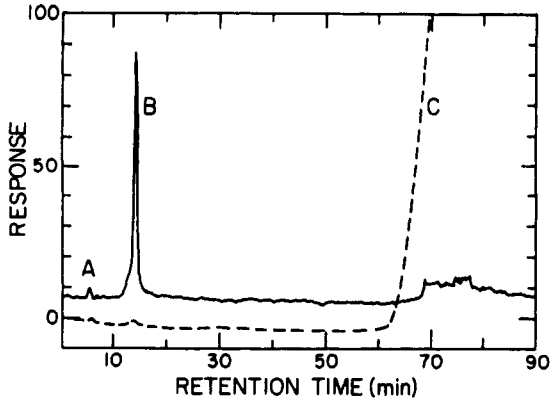

Figure 1. Size exclusion chromatography trace for the crude product containing Py–PEO and Py–PEO–Py: flow rate, 1.0 mL/min; injected volume, 200 μL; fluorescence detector, λ_{exci} = 342 nm, λ_{emi} = 520 nm; (- - -) fluorescence detector; (—) refractive index detector.

over a period of days to weeks in a desiccator, and thus should be used soon after preparation.

Pyrene-Labeled PEO. Poly(ethylene oxide) (1.44 g, M_n = 8000, M_w/M_n = 1.08, Aldrich) was dried by dissolving it in toluene followed by solvent removal at reduced pressure, and then dissolved in dry THF (10 mL). Under a nitrogen atmosphere, a piece of potassium metal (0.48 g) was added to the solution. After the solution was stirred for ca. 1 h (the solution was pale yellow), the remaining potassium was removed with a tweezer, and a solution of 3 (348 mg) in dry THF (5 mL) was added. The solution was heated to 55 °C for 10 h. 2-Propanol (5 mL) was added, and then all solvent was removed on the rotary evaporator. The crude product was treated with diethyl ether to remove non-PEO-bound organic material. After filtering, the solution was dried and analyzed by size exclusion chromatography (SEC) both in water and in THF. In THF one observes one peak essentially identical to that of the starting PEO, but now showing bound pyrene by UV detection.

Purification of Pyrene-Labeled PEO. SEC analysis of the polymer in aqueous solution using a TSK G3000 PW column showed three peaks (cf. Results and Discussion and Figure 1), corresponding, in increasing elution time, to PEO, Py–PEO, and Py–PEO–Py. It was possible by successive extraction–back-extraction steps using 50-mL quantities of CH_2Cl_2 and water to obtain a sample of Py–PEO–Py almost free of Py–PEO. This is the material used in our earlier publication.[10] The dried CH_2Cl_2 solution was treated with activated charcoal, filtered, and concentrated, and the polymer was freeze-dried from benzene to yield a white powder.

For the work described here, samples eluting off the SEC column in water were collected, reinjected for analysis, and used directly for the fluorescence experiments. In this way samples of Py–PEO free of Py–PEO–Py and of Py–PEO–Py free of Py–PEO were obtained. The purity of Py–PEO–Py could be checked by showing in a fluorescence decay experiment that there was less than 0.1% of any pyrene-containing species with a lifetime corresponding to Py–PEO.

Dynamic and Static Fluorescence Measurements. Fluorescence spectra were obtained on a SPEX Fluorolog 112 spectrometer. Decay curves were obtained by the time-correlated single-photon counting (SPC) technique. The excitation source was a coaxial flash lamp (Edinburgh Instruments Model 199F). The excitation wavelength was selected by a Jobin-Yvon Model H-20 monochromator, and that of the fluorescence by a SPEX Minimate Model 1760 monochromator. The analysis of the excited monomer and excimer decay curves was performed with the δ-pulse convolution method. Reference decay curves of degassed solutions of BBOT [2,5-bis(5-*tert*-butyl-2-benzoxazolyl)thiophene] in ethanol (τ = 1.47 ns) and POPOP [1,4-bis(5-phenyloxazol-2-yl)benzene] in cyclohexene (τ = 1.1 ns) were used for analysis of the excimer and monomer decay curves, respectively. For SPC fluorescence measurements, the excitation wavelength was 342 nm, the monomer fluorescence was observed at 374 nm, and the excimer fluorescence was observed at 520 nm.

Table I
Retention Times for Different Methanol Concentrations (wt %) in the Mobile Phase with a TSK G3000 PW Column and a 1.5 mL/min Flow Rate[a]

MeOH concn (wt %)	retention time (peak B) (min)	retention time (peak C) (min)
0	11	75
20	7	13
27	6	9

[a] The absorption for the pyrene monomer was monitored at 342 nm.

For steady-state measurements, the excitation wavelength was 342 nm and the intensity of the monomer was obtained by integrating the fluorescence emission over 371–386 nm. The intensity of the excimer was measured by integration over 450–550 nm of the area obtained after substracting the normalized monolabeled polymer fluorescence spectrum from the fluorescence spectrum of the solution under study.

Results and Discussion

Esters of pyrenebutyrate hydrolyze slowly in water. This hydrolysis adds a serious uncertainty factor to the study of pyrene-end-capped PEO in water and in alcohol solvents when the pyrene is attached as an ester. Of course if one carries out proper controls and works quickly, this problem can be neglected. Nevertheless, there are experiments which require a stable linkage and there are times when one needs to have material containing exactly 2.0 pyrenes per chain.

We chose to prepare Py–PEO–Py using an ether linkage to attach the pyrenes. The chemistry of the ether synthesis is straightforward, whereas the purification of the products is sufficiently interesting to merit some discussion.

The pyrene-end-capped PEO elutes from the TSK G3000 PW SEC column well past the solvent peak of the column (cf. Figure 1). We suspected that adsorption of the chain ends to the column packing material was occurring. This is the kind of interaction one would observe with a standard reversed-phase HPLC column. This explanation is confirmed by monitoring the effect of methanol in the eluent on the retention times (cf. Table I). The PEO itself is detected only by the RI detector, whereas Py–PEO and Py–PEO–Py are also detected by their UV absorption at 342 nm. It is the doubly-labeled chain which is most sensitive to the presence of added methanol in the system.

With this analytical tool to monitor the results, one can obtain nearly pure Py–PEO–Py by artful use of extraction and back-extraction using CH_2Cl_2 and water. An automated countercurrent distribution method would be preferable. Since we needed such small quantities for these experiments and also wanted a sample of Py–PEO for comparison, we collected fractions of Py–PEO and of Py–PEO–Py as they eluted from the analytical SEC column using pure water or water–methanol as the eluent.

Fluorescence spectra of Py–PEO and of Py–PEO–Py in water are shown in Figure 2. There is no excimer emission in the spectrum of the former, and a strong excimer band in the spectrum of the latter. Deaerated solutions of both samples give for the monomer simple exponential fluorescence decay profiles under all conditions examined here. Their lifetimes are significantly different, and in the absence of quencher have the values τ_{Py-PEO} = 219 ns and $\tau_{Py-PEO-Py}$ = 166 ns. The latter sample shows no trace of a long-tail component in its decay. Careless sample handling can lead to chain oxidation and cleavage, and the presence of singly labeled polymer is immediately apparent in a fluorescence decay experiment. The ex-

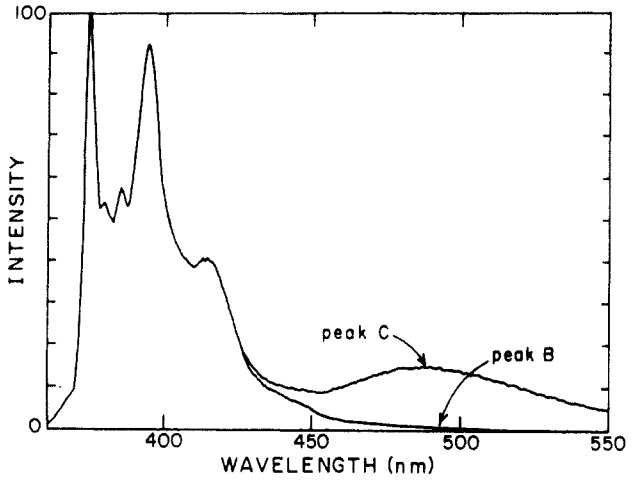

Figure 2. Fluorescence spectra of Py–PEO and Py–PEO–Py in water at 10^{-6} M.

Scheme I

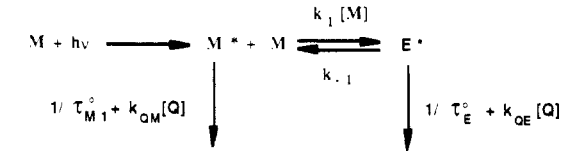

Scheme II

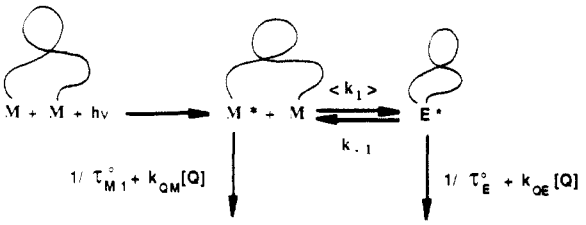

ponentiality of the monomer decay profile in Py–PEO–Py is good evidence that no excimer dissociation to reform monomer can be detected in our experiments.

Traditional Kinetic Models. When a quencher [Q] is added to a system undergoing excimer formation, the intensities of both the monomer emission (I_M) and excimer emission (I_E) are affected. The kinetics of these reactions are normally described in terms of Scheme I. Here the excimer E* is formed by encounter of photoexcited M* with M with a rate described by k_1[M], and the excimer dissociation rate is described by k_{-1}. The terms $k_M = (\tau_{M1}^0)^{-1}$ and $k_E = (\tau_E^0)^{-1}$ refer to the unquenched decay rates of M* and E*, respectively. The subscript M1 refers to the monomer of Py–PEO.

In terms of Scheme I and in a static experiment, the following two differential equations describe the decay of monomer and excimer concentrations:

$$d[M^*]/dt = I^0 - (k_M + k_1[M] + k_{QM}[Q])[M^*] + k_{-1}[E^*] = 0 \quad (1)$$

$$d[E^*]/dt = -(k_E + k_{-1} + k_{QE}[Q])[E^*] + k_1[M][M^*] = 0 \quad (2)$$

where I^0 refers to the light intensity absorbed by the sample. From eq 2 one derives the ratio I_E/I_M given in eq 3. We are concerned with intramolecular excimer formation and emission for the case of two pyrenes attached to the ends of a long polymer chain. Under our experimental conditions (23 °C) we have good evidence that excimer dissociation makes an insignificant contribution to the reaction kinetics. We rewrite Scheme I, setting $k_{-1} = 0$ and replacing k_1[M] with a first-order rate constant $\langle k_1 \rangle$, where the angular brackets indicate that this term represents an average over the (narrow) distribution of end-to-end distances in the sample.

$$\frac{I_E}{I_M} = \frac{[E^*]}{[M^*]} = \frac{k_1[M]}{k_E + k_{-1} + k_{QE}[Q]} \quad (3)$$

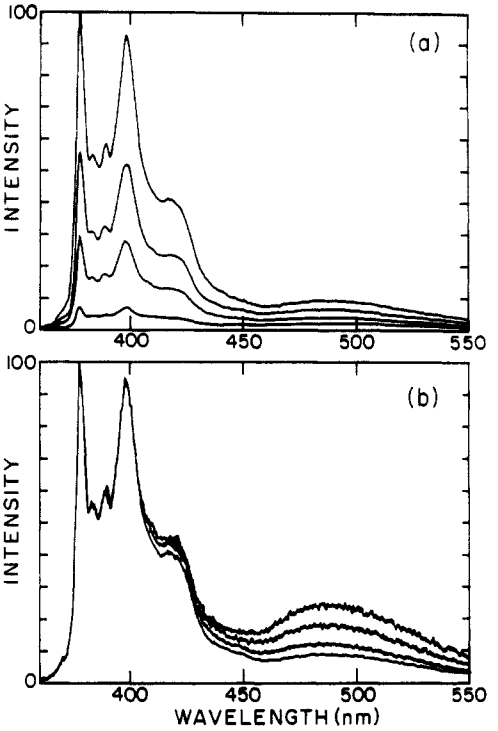

Figure 3. Fluorescence spectra of 10^{-6} M Py–PEO–Py in water in the presence of increasing concentrations of NaI: (a) non-normalized spectra, from top to bottom, $[I^-] = 0.0$ M, 3.49×10^{-3} M, 1.04×10^{-2} M, and 6.6 t 10^{-2} M; (b) spectra normalized at the (0, 0) band of pyrene fluorescence (374 nm), from top to bottom, $[I^-] = 6.6 \times 10^{-2}$ M, 1.04×10^{-2} M, 3.49×10^{-3} M, and 0.0 M.

In terms of Scheme II, two relatively simple expressions describe the quenching of I_M and of I_E as a function of quencher concentration:

$$I_M^0/I_M = 1 + k_{QM}\tau_{M2}^0[Q] \quad (4)$$

with

$$\tau_{M2}^0 = (\langle k_1 \rangle + k_M)^{-1} \quad (5)$$

and

$$I_E^0/I_E = (1 + k_{QE}\tau_E^0[Q])(1 + k_{QM}\tau_{M2}^0[Q]) \quad (6)$$

The subscript M2 refers to the monomer of Py–PEO–Py. Equations 3, 4, and 6 make the following predictions about the effect of quencher on the steady-state fluorescence intensities of M* and E* relative to their values (I_M^0, I_E^0) in the absence of quencher. First, we expect a linear dependence of I_M^0/I_M on [Q] for both Py–PEO and Py–PEO–Py. The former species should exhibit a steeper slope ($k_{QM}\tau_{M1}^0$) because of its longer lifetime than that ($k_{QM}\tau_{M2}^0$) obtained from Py–PEO–Py. Excimer quenching should lead to a plot of I_E^0/I_E which is concave upward, since, at elevated quencher concentrations, this ratio becomes proportional to $[Q]^2$. Finally, eq 3 predicts that in the presence of an increasing quencher concentration I_E/I_M will decrease. If k_{QE} were equal to zero, then I_E^0/I_E would increase linearly with [Q] and I_E/I_M would remain constant.

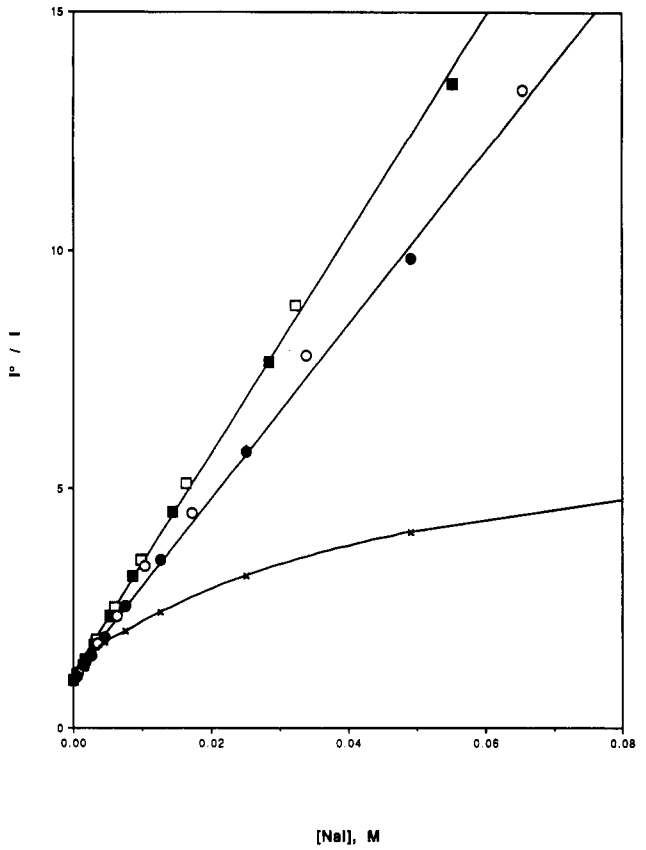

Figure 4. Stern–Volmer plots for iodide quenching of Py–PEO fluorescence and for quenching of the monomer and excimer fluorescence of Py–PEO–Py: (□) $\tau_{M1}^{\circ}/\tau_{M1}$, (■) I_{M1}°/I_{M1}, (●) $\tau_{M2}^{\circ}/\tau_{M2}$, (○) I_{M2}°/I_{M2}, (×) I_E°/I_E.

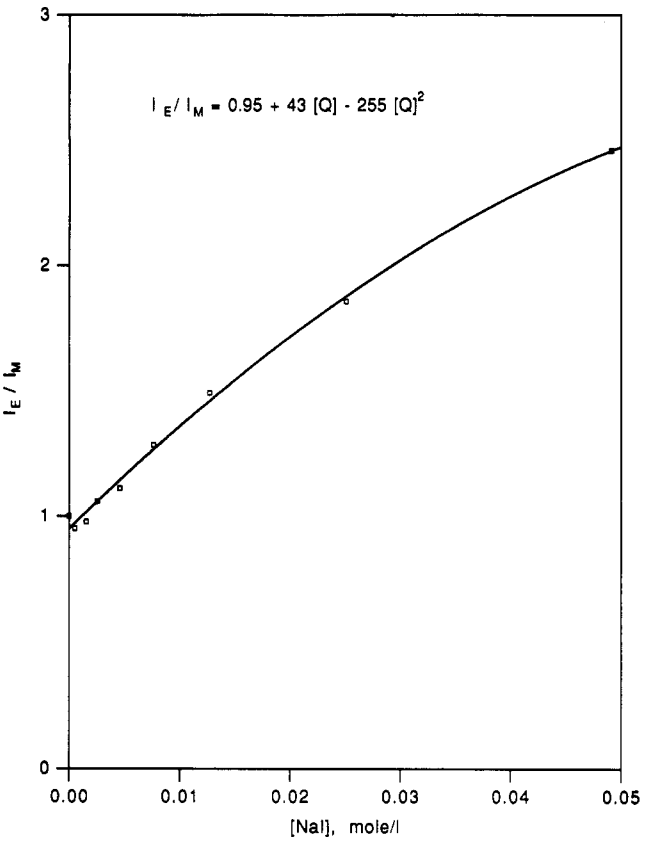

Figure 5. I_E/I_M vs $[I^-]$ for Py–PEO–Py in water.

In the following section we examine experiments involving dilute aqueous solutions of Py–PEO–Py and Py–PEO. We find that monomer quenching does satisfy eq 4, but that excimer quenching is completely inconsistent with eqs 3 and 6.

Quenching Experiments. In the presence of NaI, both monomer and excimer bands of aqueous Py–PEO–Py are quenched. An example is shown in Figure 3 where the fluorescence spectra in the presence of different concentrations of I^-, ranging from 0.0 to 0.066 M, are compared to that in the absence of quencher.

In Figure 4 we show Stern–Volmer plots for both monomer and excimer quenching. The uppermost line refers to Py–PEO. Here we show both intensity data I_M°/I_M and lifetime data $\tau_{M1}^{\circ}/\tau_{M1}$ where τ_{M1} refers to the monomer fluorescence lifetime when quencher is added to the solution. Note that both sets of data fit the expression

$$\tau_{M1}^{\circ}/\tau_{M1} = I_{M1}^{\circ}/I_{M1} = 1 + k_{QM}\tau_{M1}^{\circ}[Q] \qquad (7)$$

where yields a k_{QM} value of $1.04 \times 10^9\ M^{-1}\ s^{-1}$. The second line refers to experiments involving Py–PEO–Py. Here, too, both intensity data and lifetime data $\tau_{M2}^{\circ}/\tau_{M2}$ fit an expression analogous to eq 7, with τ_{M2} and τ_{M2}° replacing τ_{M1} and τ_{M1}°. With this data we calculate $k_{QM} = 1.10 \times 10^9\ M^{-1}\ s^{-1}$, essentially identical to that found for the quenching of Py–PEO fluorescence by I^-.

In these experiments we did not originally keep ionic strength constant. We therefore examined the fluorescence of Py–PEO and Py–PEO–Py as a function of NaCl concentration in water. Even at the highest salt concentration [0.06 M], there was no effect on their fluorescence intensities or spectra.

At the bottom of Figure 4 we plot I_E°/I_E vs $[I^-]$ for Py–PEO–Py. Instead of finding upward curvature as predicted by eq 5, the plot curves downward, as though it might level off at elevated [Q].

To emphasize this discrepancy between the predictions of traditional models and our observations, we plot I_E/I_M vs $[I^-]$ in Figure 5. *Here we anticipate a decrease in I_E/I_M (cf. eq 3) and observe an increase in this ratio.*

Kinetic Model Including Preassociated Pairs. The excimer intensity in Py–PEO–Py is sufficiently weak that it is difficult to obtain accurate $I_E(t)$ intensity profiles. These measurements demonstrate unambiguously that much of the excimer intensity is formed within the first nanosecond of the lamp pulse. An example is shown in Figure 6. This type of behavior has been observed previously for PEO end-capped with pyrenebutyrate ester groups and in other water-soluble polymers bearing pyrene pendant groups. The essentially instantaneous excimer emission has been attributed to the presence of preassociated pyrene pairs.[8,12] Such pairs are very rare in organic solvents.[17] In water hydrophobic effects promote end group pairing. This interaction is opposed by the cyclization entropy of the chain.

On the basis of these considerations we modify Scheme II to include a fraction of chains α which have their pyrene end groups preassociated, in equilibrium with the remaining fraction $(1 - \alpha)$ having nonassociated ends.

In Scheme III we assume equal probability of light absorption by the preassociated and free end groups, generating an equivalent fraction of species M* and E*. Our model also presumes that the excimers produced on direct pair excitation (E^*_{assoc}) and formation through diffusion (E^*_{diff}) are identical. There is good evidence, based upon picosecond time-resolved fluorescence spectra measurements[13] on pyrene-labeled (hydroxypropyl)cellulose, that this assumption is valid. This model is also

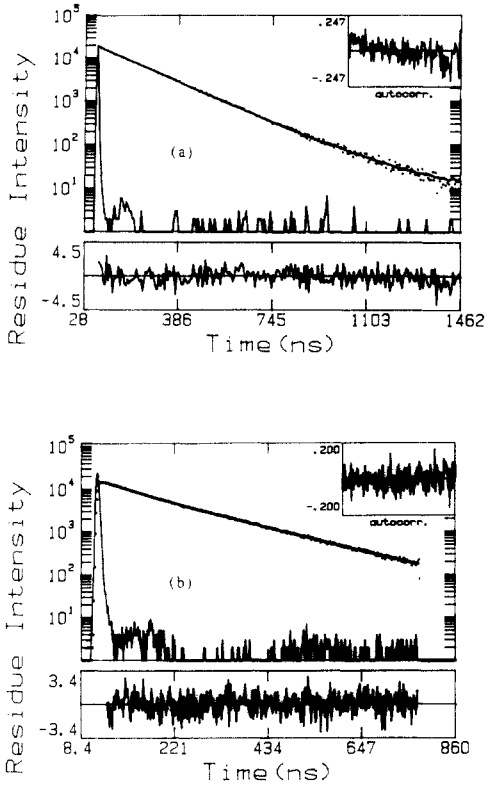

Figure 6. Fluorescence decay profile of (a) the monomer and (b) the excimer emission for Py–PEO–Py in water: λ_{exci} = 342 nm, $\lambda_{emi}^{monomer}$ = 374 nm, and $\lambda_{emi}^{excimer}$ = 520 nm.

consistent with the large amount of prompt excimer emission observed by us and others.

Under conditions where $k_{-1} = 0$, Scheme III leads to the following expressions appropriate for steady-state fluorescence experiments:

$$d[M^*]/dt = (1-\alpha)I^o - ((\tau_{M1}^o)^{-1} + \langle k_1\rangle + k_{QM}[Q])[M^*] = 0 \quad (8)$$

$$d[E^*_{diff}]/dt = \langle k_1\rangle[M^*] - ((\tau_E^o)^{-1} + k_{QE}[Q])[E^*_{diff}] = 0 \quad (9)$$

$$d[E^*_{assoc}]/dt = \alpha I^o - ((\tau_E^o)^{-1} + k_{QE}[Q])[E^*_{assoc}] = 0 \quad (10)$$

$$[E^*] = [E^*_{assoc}] + [E^*_{diff}] \quad (11)$$

The set of equations gives the following expression for I_E^o/I_E:

$$\frac{I_E^o}{I_E} = \frac{(1 + k_{QE}\tau_E^o[Q])(1 + k_{QM}\tau_{M1}^o[Q])(\langle k_1\rangle + \alpha k_M)}{(\langle k_1\rangle + \alpha k_M + \alpha k_{QM}[Q])} \quad (12)$$

For I_E/I_M

$$\frac{I_E}{I_M} = \frac{I_E^o}{I_M^o}\left(1 + \frac{\alpha k_{QM}\tau_{M1}^o}{\alpha + \langle k_1\rangle\tau_{M1}^o}[Q]\right)(1 + k_{QE}\tau_E^o[Q])^{-1} \quad (13)$$

The superscript o in eqs 12 and 13 refers to the fluorescence intensities of M* and E* in a solution without quencher. The terms in parentheses in eq 13 can be expanded as a polynomial. Keeping terms to second order,

Scheme III

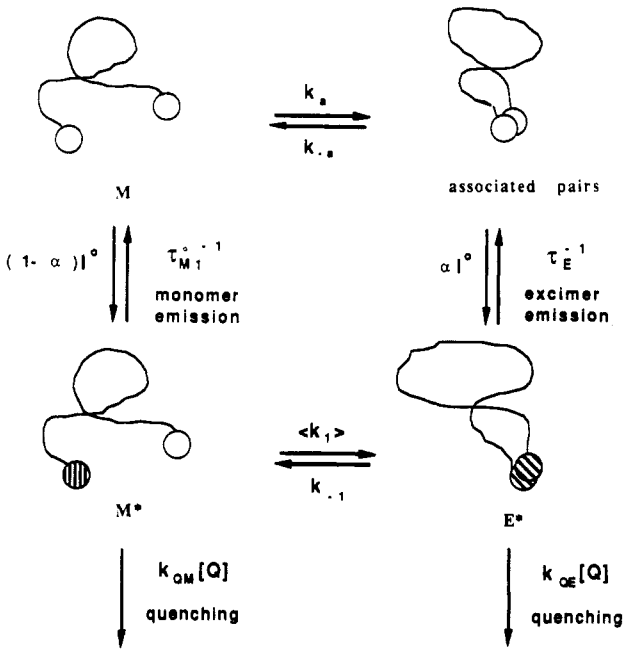

we obtain

$$\frac{I_E}{I_M} = \frac{I_E^o}{I_M^o}(1 + A[Q] + B[Q]^2 + ...) \quad (14)$$

where A and B are given by

$$A = \frac{k_{QM}\tau_{M1}^o}{1 + (1/\alpha)\langle k_1\rangle\tau_{M1}^o} \quad (15a)$$

$$B = -k_{QE}\tau_E^o A \quad (15b)$$

The curve in Figure 5 gives an excellent fit to the quadratic expression of eq 14, yielding

$$\frac{I_E}{I_M} = \frac{I_E^o}{I_M^o}(1 + 43.4[Q] - 255[Q]^2) \quad (16)$$

With these values of A and B, we are able to obtain the magnitude of α and comment on the relative quenching efficiency of I^- for monomers and excimers. From lifetime measurements we obtain $\langle k_1\rangle = 1.17 \times 10^6\ s^{-1}$. From the data in Figure 4 we obtain $k_{QM} = 1.05 \times 10^9\ M^{-1}\ s^{-1}$, typical of diffusion-controlled bimolecular rate constants for electron transfer quenching of pyrene by an electron donor in water.[14] Since τ_M is known (219 ns), we have two equations and two unknowns, and from A and B we obtain $\tau_E k_{QE} = 5.9\ M^{-1}$ and $\alpha = 0.07$. Thus, we learn that, for the polymer studied at 23 °C, 7% of the chains have their pyrene groups preassociated prior to excitation.

Pyrene excimer lifetimes are typically in the range of 50–60 ns. This decay is not discernable in the $I_E(t)$ profile shown in Figure 6. This profile contains a superposition of the emission decay of D* formed essentially instantaneously, and the growth and decay of E* formed dynamically. Under normal circumstances when the excimer formation rate is slower than its decay, it is the formation rate which dominates the decay part of the $I_E(t)$ profile.[4] Thus, the characteristic rate calculated from the $I_E(t)$ decay shown in Figure 6 is essentially equal to that of the $I_M(t)$. This result establishes that the $I_M(t)$ profile in Figure 6 provides information about the rate of formation of E* from M*, but nothing about the excimer lifetime.

To estimate a value for k_{QE}, we assume that τ_E^o is approximately equal to 60 ns. Thus, k_{QE} has a magnitude

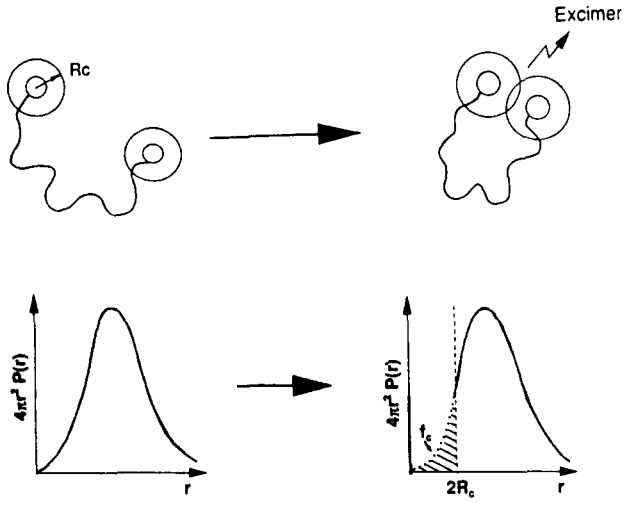

Figure 7. Schematic diagram for the consideration of hydrophobic attraction and the modified probability distribution function of the end-to-end distance.

on the order of 1×10^{-8} M^{-1} s^{-1}, nearly a factor of 10 smaller than k_{QM}. One of the reasons our experiment works so well is that iodide is a much poorer quencher of the pyrene excimer than it is of locally excited pyrene.

We are now in a position to explain the excimer quenching plot given by the lowermost curve in Figure 4. The initial slope at low [Q] is identical to that of I_M°/I_M for Py–PEO–Py, indicating that the initial slope is dominated by the $k_{QE}\tau_E^\circ$ term in the numerator of eq 13. At high [Q] where $\alpha k_{QM}[Q] \gg \langle k_1 \rangle + \alpha k_M$, eq 13 simplifies to

$$\frac{I_E^\circ}{I_E} = k_{QE}\tau_E^\circ[Q]\left[\frac{\langle k_1 \rangle + \alpha k_M}{\alpha\langle k_1 \rangle + \alpha k_M}\right] \qquad (17)$$

The term in brackets takes the value 3.7 which means that, in the limit of large [Q], the plot in Figure 4 will be linear with a slope equal to $3.7k_{QE}\tau_E^\circ$. This is what is observed. If α were equal to zero, eq 13 would predict a $[Q]^2$ dependence in I_E/I_M derived for large [Q] as expected from Scheme II (eq 5).

Cyclization Probability. Several years ago Char et al.[8b] proposed a model for cyclization in water of PEO containing Py as hydrophobic end groups. In their view, the hydrophobic groups interact over a certain capture distance $2R_c$ (see Figure 7) to perturb the normalized probability density function of end-to-end distances $P(r,N)$ for the chain. The fraction of preassociated pyrene ends is

$$f_c = \alpha = \int_0^{2R_c} 4\pi r^2 P(r,N)\, dr \qquad (18)$$

and the modified mean-squared end-to-end distance after taking account of the captured ends is

$$\langle R^2 \rangle = (1 - f_c)\int_{2R_c}^{\infty} 4\pi r^4 P(r,N)\, dr \qquad (19)$$

This model can be evaluated quantitatively if the form of $P(r,N)$ is known. Char et al.[7b] derived an analytic expression for f_c and $\langle R^2 \rangle$ assuming a Gaussian form for $P(r,N)$. While this is appropriate for a Θ solvent, for PEO in water, a good solvent, it neglects the correlation hole in $P(r,N)$ for small r.[15] Our experiments in other systems[16] suggest that excluded volume effects can cause nearly an order of magnitude decrease in f_c. Nevertheless, our most important result in the work reported here is that we provide strong support for the two-state model proposed by Char et al. and shown in Figure 7. If values of $\alpha = f_c$ can be obtained for Py–PEO–Py samples varying in chain length, the chain length dependence of the cyclization probability in such a system could be evaluated.

Implications

It is interesting to note that some pyrene-end-capped oligomers show a tendency for ground-state association in organic solvents such as chloroform and toluene.[17] These oligomers, however, have much shorter chain lengths than the polymer we deal with in the present study. Nevertheless, even in organic solvents, such association was correlated with the Hildebrand solubility parameter. Furthermore, recent experiments from Rohm and Haas[12] on model associative thickeners in which pyrene is incorporated into the hydrophobic end groups have shown a transition with increasing dilution of the system. This transition, from inter- to intramolecular excimer formation resembles that observed several years ago by Oyama et al.[7a] If one wishes to understand the association process in more detail, it is essential to have an appropriate methodology for evaluating kinetic data in terms of a model. Char et al.[8b] have proposed a model for the case of intramolecular end group association for water-soluble polymers bearing hydrophobic substituents. Until now, the steady-state and fluorescence decay data seemed too complex to lend themselves to a quantitative analysis.

Our contribution here is to provide a methodology for interpreting these experiments. This methodology will need some modifications, to take into account, for example, hypochromic effects which will lower the extinction coefficient of the preassociated pyrene pair relative to that of free pyrene. A reviewer commented that we went to a lot of trouble to establish that only 7% of the pyrene end groups are preassociated prior to excitation. The amount of preassociation will increase with decreasing chain length, and also increase with increasing hydrophobicity of the end groups. Extending this analysis to intermolecular end group association remains an elusive goal. We hope to take steps in this direction in the future.

References and Notes

(1) (a) Schulz, D. N., Glass, J. E., Eds. *Polymers as Rheology Modifiers*; ACS Symposium Series 462; American Chemical Society: Washington, DC, 1991. (b) Noward, P. R.; Leasure, E. L.; Rosier, S. T.; Schaller, E. J. *J. Coat. Technol.* **1992**, *64* (804), 87.
(2) For reviews, see: (a) Chu, D. Y.; Thomas, J. K. In *Photochemistry and Photophysics*; Rubek, J. F., Ed.; CRC Press: Boca Raton, FL, 1991; Vol. III. (b) Zana, R. *Surfactant Solutions*; Marcel-Dekker: New York, 1987.
(3) Cuniberti, C.; Perico, A. *Eur. Polym. J.* **1977**, *13*, 369.
(4) Birks, J. B. *Photophysics of Aromatic Molecules*; Wiley-Interscience: New York, 1971.
(5) Winnik, M. A. *Acc. Chem. Res.* **1985**, *18*, 83.
(6) Cheung, S. T.; Winnik, M. A.; Redpath, A. E. C. *Makromol. Chem.* **1982**, *183*, 1815.
(7) (a) Oyama, H. T.; Tang, W. T.; Frank, C. W. *Macromolecules* **1987**, *20*, 474, 1839. (b) Hemker, D. J.; Frank, C. W. *Macromolecules* **1990**, *23*, 4404. (c) Hemker, D. J.; Garza, V.; Frank, C. W. *Macromolecules* **1990**, *23*, 4411.
(8) (a) Char, K.; Frank, C. W.; Gast, A. P.; Tang, W. T. *Macromolecules* **1987**, *20*, 1833. (b) Char, K.; Frank, C. W.; Gast, A. P. *Macromolecules* **1989**, *22*, 3177.
(9) Char, K.; Gast, A. P.; Frank, C. W. *Langmuir* **1988**, *4*, 989.
(10) Hu, Y. Z.; Zhao, C. L.; Winnik, M. A.; Sundaranajan, P. R. *Langmuir* **1990**, *6*, 880.
(11) Akiyama, S.; Nakasuji, K.; Nakagawa, M. *Bull. Chem. Soc. Jpn.* **1971**, *44* (8), 2231.
(12) Richey, B.; Kirk, A. B.; Eisenhart, E. K.; Fitzwater, S.; Hook, J. *J. Coat. Technol.* **1991**, *63* (798), 31.

(13) Yamazaki, I.; Winnik, F. M.; Winnik, M. A.; Tazuke, S. *J. Phys. Chem.* **1987**, *91*, 4213.
(14) (a) Shizuka, H.; Nakamura, M.; Morita, T. *J. Phys. chem.* **1980**, *84*, 989. (b) Masuhara, H.; Shioyama, H.; Saito, T.; Hamada, K.; Yasoshima, S.; Mataga, N. *J. Phys. Chem.* **1984**, *88*, 5868.
(15) de Gennes, P. G. *Scaling Concepts in Polymer Physics*; Cornell University Press: Ithaca, NY, 1979; Chapter 1.
(16) (a) Winnik, M. A.; Li, X. B.; Guillet, J. E. *J. Polym. Sci., Polym. Symp. Ed.* **1985**, *73*, 113. (b) Martinho, J. M. G.; Winnik, M. A. *Macromolecules* **1986**, *19*, 2281. (c) See also: Winnik, M. A. In *Molecular Dynamics in Restricted Geometries*; Klafter, J., Drake, J. M., Eds.; Wiley: New York, 1989; Chapter 8.
(17) (a) Reynders, P.; Kühnle, W.; Zachariasse, K. A. *J. Am. Chem. Soc.* **1990**, *112*, 3929. (b) Reynders, P.; Kühnle, W.; Zachariasse, K. A. *J. Phys. Chem.* **1990**, *94*, 4073.

Registry No. 2, 144269-60-3.